Josephson Junction Oscillator Arrays

Matthew J. Lewis, Dale Durand, and Andrew D. Smith
TRW Space & Technology Group.

Peter Hadley*
Stanford University

Abstract

We have studied the stability and coherence of distributed Josephson junction array oscillators both theoretically, and experimentally. Distributed Josephson oscillator arrays successfully operate above 300 GHz with microwatt power levels.[1] The use of wavelength-long transmission lines between Josephson elements has overcome lithographic and stability difficulties plaguing earlier compact designs. In this paper, we study the dynamic stability and phase coherence of Josephson arrays.

We have extended lumped array stability analysis[2] both for more realistic embedding environments and to distributed arrays including element to element time delays. Stable oscillator operation in lumped arrays depends on both junction and drive parameters. Wide ranges of embedding impedances provide coherent output oscillations. For distributed arrays, the available oscillator output power increases with the total array size. These results are in good agreement with experimental observations.[1]

Experimentally, we have fabricated and operated a distributed array oscillator and observed at least 50 nW of power at 125 GHz using an on-chip detection circuitry.

Introduction

There is an increasing need for sub-millimeter wave sources for a wide range of applications ranging from astronomy to communications. Single Josephson junction oscillators have been successfully operated at frequencies up to hundreds of GHz, but these single junctions do not produce adequate power and have very low output impedance. Both of these limitations can be overcome by placing many junctions in a series array.

Early work in Josephson oscillator arrays concentrated on tightly spaced series arrays of junctions[3]. Workers quickly discovered successful high power operation of these arrays centered around obtaining

coherent, in-phase operation of the individual oscillator elements. Although the series array geometry imposes a uniform current requirement on the junctions, the oscillation voltages of the Josephson elements tend to destructively interfere unless specific feedback conditions are maintained.

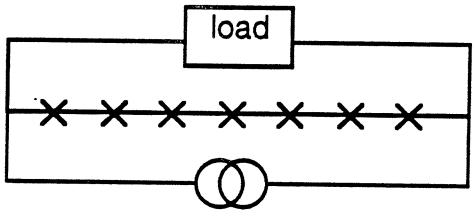

Figure 1. Lumped element Josephson array. Each cross represents an ideal Josephson element, shunt resistor, and shunt capacitance.

Hadley[2] and Jain et al[3] have studied electrically short, Josephson series arrays. (See Fig. 1). Coherent operation depends on the external load element(s), which provide feedback to the individual array elements. Hadley found separate parameter ranges leading to chaotic or very stable, coherent array operation, depending upon junction capacitance, critical current, bias current, and load.

These models, however, have their limitations. They neglect the parasitic inductance between junctions, as well as capacitance to ground of interconnecting lines. At low frequencies and for array lengths much shorter than a wavelength, these effects should be minimal. For sub-millimeter, microwatt oscillators these additional elements dominate the circuit dynamics.

In experimental work at Stony Brook, Wan, et al.[1] cleverly side-stepped the issue of long-array parasitics. Since interconnection wiring is unavoidable between Josephson elements, the Stony Brook design chooses the transmission line interconnection length to be precisely one oscillation wavelength long. (See Fig. 1.) Electrically, the transmission line appears identical to a zero-length interconnect for all frequencies which are multiples of the fundamental. Thus for any multiple of the fundamental frequency, solutions of the tightly-spaced array oscillator should also apply to the Stony Brook design array.

In this theoretical study we have extended the analyses for the lumped element array to include the reactance of the load. This analysis only applies to long arrays when the interconnects between the junctions are one wavelength long. We also consider more general distributed arrays. Here we find a

picture significantly more complex than simple wavelength arguments would predict. Some coherent solutions appear for operating frequencies which are a fraction of the junction spacing. In addition, some parameter choices which give stable short array solutions lead to out-of-phase solutions in Stony Brook array geometries.

Stability Theory for Oscillators

In-phase solution, where all of the junctions oscillate with the same frequency and phase, is an exact solution to the lumped element model for the arrays. Unless certain device parameter requirements are met, the in-phase solution is unstable and the oscillator will quickly decay into out-of-phase or aperiodic solutions. Previously simulations have been performed for junction arrays have been performed with a variety of β_c, current biases, and loads.[2] They show that the phase locking was strongest when $\beta_c \approx 1$ independent of the load. We were able to reproduce the earlier work and have extended it by calculating stability exponents for β_c as a function of load impedance. The equations of motion for the oscillator array are given by the conservation of current,

$$\beta_c \ddot{\varphi}_k(t) + \dot{\varphi}_k + \sin(\varphi_k(t)) + I_L(t) = I_B$$

and the voltage across the array,

$$V(t) = \sum_{k=1}^{N} \dot{\varphi}_k(t) = F(I_L(t))$$

using the usual reduced units: measuring current in units of I_c (critical current), voltage in units of I_cR_N (normal state resistance), resistance in units of R_N, capacitance in units of $\hbar/(2eI_cR_N^2)$, inductance in units of $\hbar/(2eI_c)$, and time in units of $\hbar/2eI_cR_N$.

The stability of the in-phase solution, φ_o, may be determined by considering small perturbations about that solution. Linearizing the previous equation around the in-phase solution we have

$$\beta_c \ddot{\eta}_k(t) + \dot{\eta}_k(t) + \sin(\varphi_o(t))\eta_k + i(t) = I_B$$

$$\sum_{k=1}^{N} \dot{\eta}_k(t) = F'(I_L(t))i(t)$$

After transforming to natural coordinates, we can simplify

$$\beta_c \ddot{\zeta}_k(t) + \dot{\zeta}_k(t) + \sin(\varphi_o(t))\zeta_k = 0 \qquad k = 1, 2, \cdots, N$$

$$\beta_c \ddot{\vartheta}_k(t) + \dot{\vartheta}_k(t) + \sin(\varphi_o(t))\vartheta_k + i(t) = 0$$

$$N\dot{\vartheta}(t) = F'(I_{o(t)})i(t)$$

The first equation arises frequently in physical problems and can be analyzed using Floquet theory. There are two independent solutions to the equation for ζ which have the form $\exp(\rho t)\chi(t)$ where $\chi(t)$ is a periodic function with the same period as φ_o and ρ is called the stability exponent The two solutions to the equation for ζ form a basis from which we can form any other solution. We can choose two independent solutions ζ_a and ζ_b which have the corresponding initial conditions $\zeta_a(0)=1$, $\dot{\zeta}_a(0)=0$, $\zeta_b(0)=0$, and $\dot{\zeta}_b(0)=1$. Since $\cos(\varphi_o)$ is a periodic function, $\zeta_a(t+T)$ and $\zeta_b(t+T)$ are also solutions of the equation. We can express this as

$$\begin{pmatrix} \zeta_a(t+T) \\ \zeta_b(t+T) \end{pmatrix} = \begin{pmatrix} \zeta_a(T) & \dot{\zeta}_a(T) \\ \zeta_b(T) & \dot{\zeta}_b(T) \end{pmatrix} \begin{pmatrix} \zeta_a(t) \\ \zeta_b(t) \end{pmatrix}$$

The eigenvectors of this equation are called Floquet solutions. The corresponding stability exponents determine the stability of the perturbations. They are related to the eigenvalues, λ_j, of the matrix, by $\rho_j = \ln(\lambda_j)/T$. If both $\mathrm{Re}(\rho_1)$ and $\mathrm{Re}(\rho_2)$ are less than 0 then the perturbation decays and the solution is stable. When $\mathrm{Re}(\rho_1) = \mathrm{Re}(\rho_2) = 0$ then the solution is neutrally stable and the perturbation neither grows nor decays. In this case second order terms control the stability. If either real part is greater than zero then the solution is unstable.

Lumped-Element Simulation

Our numerical studies began with a version of SPICE[4] developed at UC Berkeley we simulated a single junction voltage controlled oscillator. We were able to relate the results of this simulation to previous experimental work done by Smith, et al[5]. Once this was successful the design was extended to multi-junction arrays. The results indicated that both the array impedance and the array voltage increased as N.

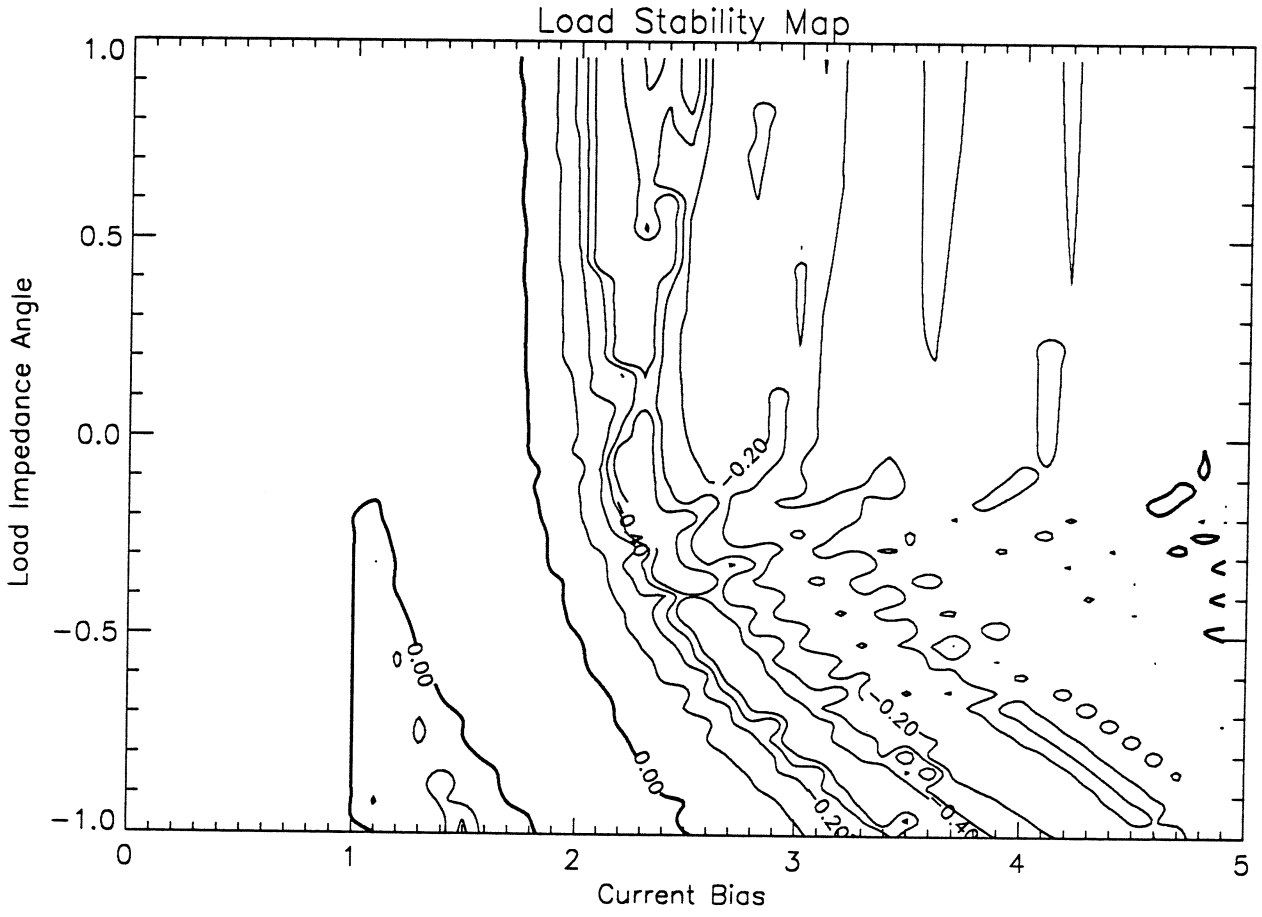

Figure 2. Floquet exponent stability plot at $\beta_c = 1.0$.

In a practical experiment, the circuit designer has good knowledge and control over internal circuit parameters of the oscillator: the critical current, shunting resistor, and junction capacitance. As a result,

tradeoffs are made to choose an appropriate β_c for stable, high power oscillation. Often it is the external load which is less well known. The oscillator design should either be unconditionally stable, or at least stable for a wide range of load impedances.

In our simulations we have chosen $\beta_c = 1.0$ in order to produce highly stable oscillations for a resistive load according to the Hadley calculations. We have then explored the dependence upon load impedance by running the simulation varying load impedance according to the following formula, parameterized by θ.

$\theta>0$ series combination of a resistor and inductor

$\theta=0$ a 1 ohm resistor

$\theta<0$ parallel combination of a resistor and capacitor

In each case, the magnitude of the impedance at the signal frequency was held fixed.

The contour plot in figure 2 shows a typical Floquet exponent map with $\beta_c = 1.0$. The more negative the exponent the greater the stability when the array is phase-locked. The results show that both resistive and partially inductive loads have wide current ranges of stable in-phase oscillation. Capacitive loads also produce stable in-phase oscillation, although over a more limited range of bias current.

The lumped element, series array has several limitations. The simple model ignores series inductance and shunting capacitance which are unavoidably present between junctions. To more realistically model circuits, a transmission line was placed between Josephson elements in our SPICE simulations. Computer runs using this model showed that the physical spacing between the elements would play a major role in the array's ability to phase-lock. Unfortunately these simulations tended to exceed certain internal time-step memory requirements of this version of SPICE.

The dynamics of widely spaced junction arrays

The distributed array oscillator of Wan, et al.[1] consists of a large number of Josephson junction oscillators, separated by transmission line, as shown in Fig. 3. Each of the Josephson junctions is separated from its neighbors by a length of transmission line. DC bias current is supplied either along the array, as shown, or in parallel to each junction.

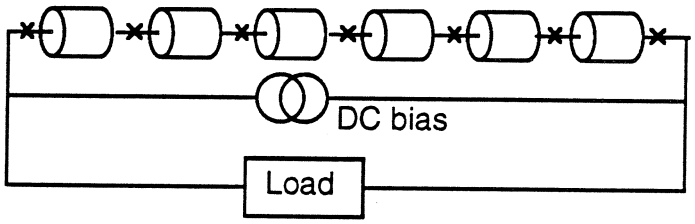

Figure 3. Distributed Josephson junction oscillator array. Identical transmission lines separate each Josephson junction.

The dynamics of the Stony Brook distributed array differs significantly from those of more tightly spaced oscillators. In the latter case, identical current passes through each oscillator element at every instant in time. Interaction between elements is rapid and quite strong. In contrast, coupling between elements of the array is moderated by the transmission lines. Each tunnel junction oscillator interacts with its nearest neighbors only after a time-of-propagation delay, τ.

In the absence of propagation losses, action of the transmission lines is straight forward to calculate. Each transmission line supports two travelling modes: right-going waves and left-going waves. (See Fig. 4.) Since action of the Josephson junction is most readily expressed in terms of a phase parameter, $\varphi(t)$, we define analogous phase quantities $\alpha(t)$ and $\beta(t)$ to describe the waveforms of the left-going and right-going waves. The time derivatives of $\alpha(t)$ and $\beta(t)$ gives the voltage waveforms at the ends of the transmission lines.

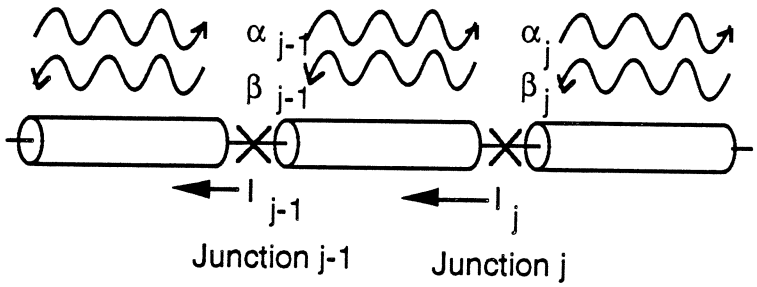

Figure 4. Detailed view of the distributed Josephson junction oscillator array. Each transmission line supports two travelling modes: a left-going wave with amplitude $\beta(t)$, and a right-going wave with amplitude $\alpha(t)$.

The equations of motion of the large array are set by current continuity conditions, voltage consistency, Josephson dynamics, and external element boundary conditions. The condition that current through each junction must simultaneously equal the current through the ends of attached transmission lines gives rise to the first set of propagation equations:

Due to the propagation delay, a waveform which begins at time $t - \tau$ at junction j-1 appears at junction j at time t.

$$I_j(t) = \Phi_0/2\pi Z_0 \, [\beta_j(t-\tau)' - \alpha_j(t)'] \tag{1}$$

$$I_j(t) = \Phi_0/2\pi Z_0 \, [\beta_{j-1}(t)' - \alpha_{j-1}(t-t)'] \tag{2}$$

where Z_0 is the transmission line characteristic impedance. Similarly the voltage at the transmission line ends depend in part on earlier generated waveforms. The voltage across each junction can be expressed as the difference in voltage between adjacent transmission lines:

$$\varphi_j' = [\alpha_j(t)' + \beta_j(t-\tau)'] - [\alpha_{j-1}(t-\tau)' + \beta_{j-1}(t)'] \tag{3}$$

In addition, the current through each junction must satisfy the Josephson equations:

$$I_j(t) = I_c \sin \varphi_j + \Phi_0/2\pi R_j \, \varphi_j' + \Phi_0 C/2\pi \, \varphi_j'' \tag{4}$$

for the RSJ model. Finally, the total current and voltage across the array must satisfy the boundary condition imposed by the external load.

$$V_{total} = \Phi_0/2\pi \ [\varphi_N' + \alpha_{N-1}(t-\tau)' + \beta_{N-1}(t)'] \qquad (5)$$

$$I_{total} = I_N$$

for an N junction array. For the special case of a resistive load, R_{ext}, this requirement becomes:

$$I_N = \Phi_0/2\pi R_{ext} \ [\varphi_N' + \alpha_{N-1}(t-\tau)' + \beta_{N-1}(t)'] \qquad (6)$$

Numerical results

We have numerically solved the dynamical equations describing oscillator junctions separated by lossless transmission lines. For a system of N identical junctions with N-1 transmission lines, the equations readily reduce to a system of N second order differential equations. We computed solutions to these equations using standard Runge-Kutta integration. In all cases we chose junction parameters and the load to produce a stable, coherent oscillation according to lumped element calculations. Results of the calculations are in qualitative agreement with Stony Brook experimental results[1], and provide interesting insight into oscillator operation.

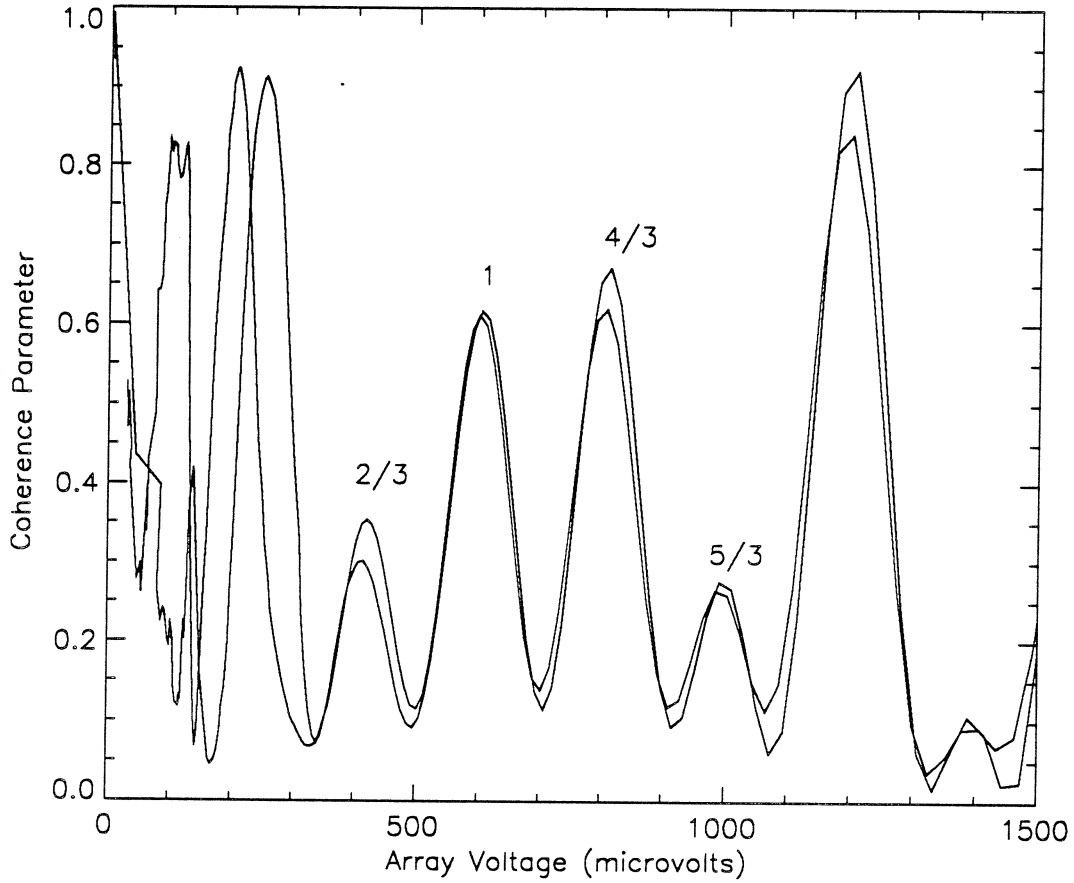

Figure 5. Numerical solution to 3 junction widely spaced junction. Fractions indicate the number of wavelengths between each junction.

Fig. 5 shows the results of a 3-junction simulation, the simplest non-trivial array. Taking account of time-of-propagation delay between junctions, we have tabulated a phase coherence parameter defined by:

$$\xi = < [\Sigma \sin (\varphi_j + j\tau)]^2 + [\Sigma \cos (\varphi_j + j\tau)]^2 > / N^2 \qquad (7)$$

where the average is taken over several oscillation cycles. This measure of phase should be one if the junctions waveforms add constructively, or less if cancellation reduces the total voltage output to a lower value.

Portions of the simulation data follow the predictions of theory. For frequencies which put precisely one oscillation wavelength between elements, the junction voltages add coherently and ξ approaches one. In

addition, the coherence parameter also is large at third sub-harmonics, where integer wavelengths fit in the *entire* array. This numerical prediction agrees with experimental observations of Wan, et al, who noted a large number of discrete frequencies of high output power.

Some aspects of the numerical simulations remain unexplained. Full phase coherence is not observed, despite the correspondence to in-phase stability in the equivalent lumped model. The reason for sub-harmonic response is yet unexplained.

Experimental Results

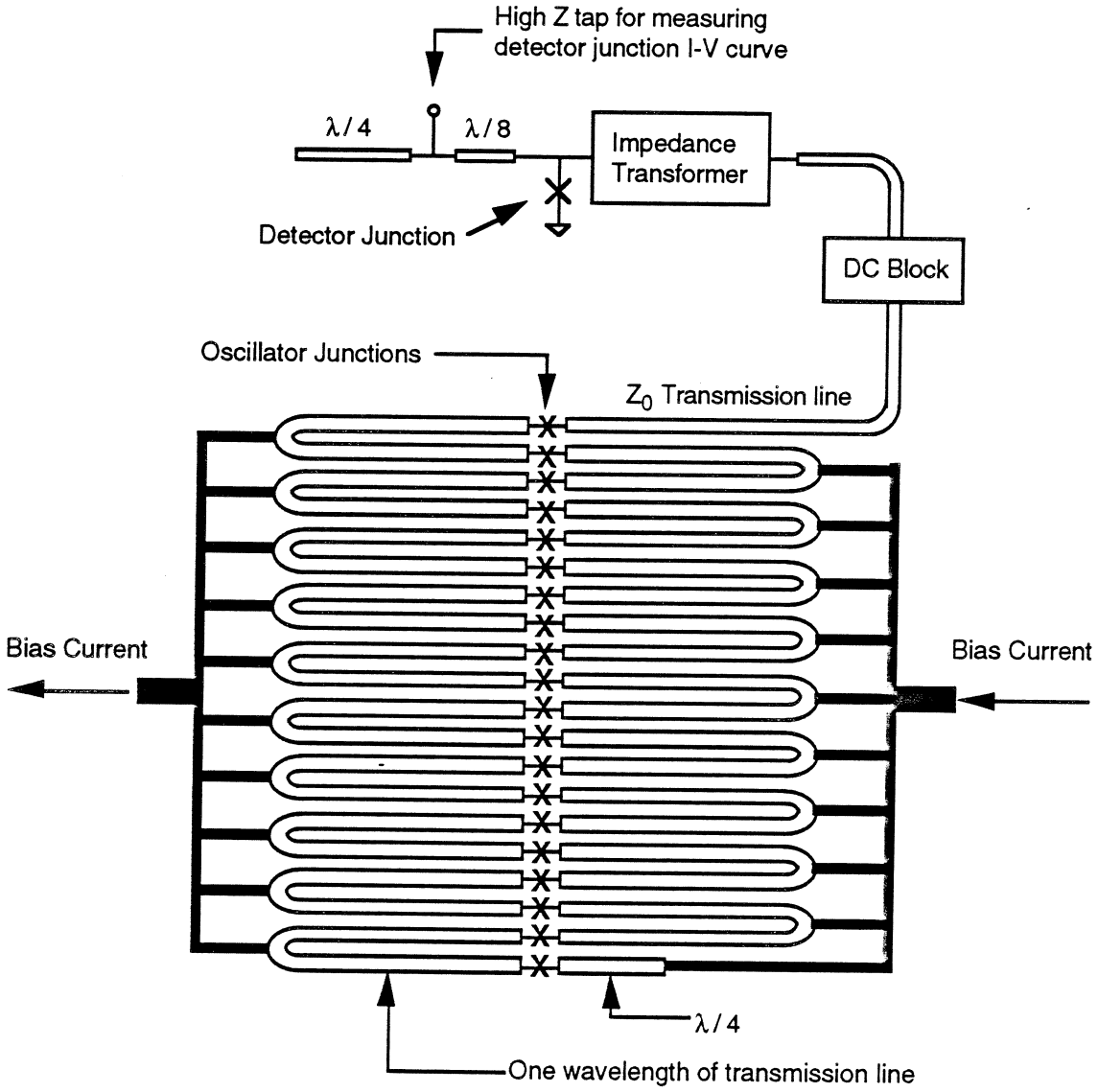

Fig. 7: A schematic diagram of the oscillator array and detection circuitry. The characteristic impedance of the line connected to the top of the array is matched to the output impedance of the array. Not shown are the damping resistors across each oscillator junction. The array is shunted by these resistors so that it can be voltage biased to produce a fixed frequency of RF.

We have fabricated and tested oscillator arrays of the general design suggested by Lukens[6]. In our tests, on-chip detection circuitry measures the RF power produced by the array. The detection circuitry consists of a Josephson junction and passive microstrip components designed to match the overall impedance of the

detector to the output impedance of the array (see Fig. 7). This method of power measurement is a realistic test of the power an array can deliver to an integrated superconducting microwave circuit.

The output of the array is fed through a DC block and an impedance matching network into a microwave detector consisting of a Josephson junction and a tuning stub. The effective conductance to the ground plane of the tuning stub cancels the shunting conductance of the junction capacitance at the operating frequency. Tuning the detector junction in this way increases its sensitivity. This kind of detector has been used successfully in the frequency range of 100 GHz.[7]

The circuit, shown in Fig. 7, is fabricated within TRW's standard Nb process based on $Nb/Al_2O_x/Nb$ junctions defined by selective anodization.[8] All the transmission lines are superconducting microstrip. The junction sizes and critical currents are within the standard range for the process used. The unshunted detector junction I-V characteristic is sharp. (See Figure 8) The oscillator junctions are 4 x 4 μm and the critical current is 1500 A/cm^2. We used these values, which are typical for our standard process, to facilitate incorporating this array design into integrated superconducting microwave circuits.

We fabricated and tested approximately 60 arrays, each with an on-chip power detection circuit as shown in Fig. 7. With the correct bias current flowing through the array, the array junctions oscillate coherently and RF induced steps in the quasi-particle portion of the detector junction I-V characteristic appear. Figure 8 shows the I-V characteristic of a detector junction with and without the array bias current on.

The steps in the quasi-particle portion of the I-V characteristic indicate power detection of approximately 100 GHz RF. We can easily estimate the minimum RF power required at the junction to produce the observed steps in the I-V curve such as those in Fig. 8 using Tucker's analysis[9]. The height of a small current step is given by $\Delta I = R \eta P$, where R is the responsivity of the junction which is at best equal to e/hf (R = 2400 A/W at 100 GHz), η is the impedance matching efficiency which is at best equal to unity, and P is the RF power incident on the junction. The RF power resulting in the step of 0.12 mA shown in Fig. 8 must be at least 0.05 μW.

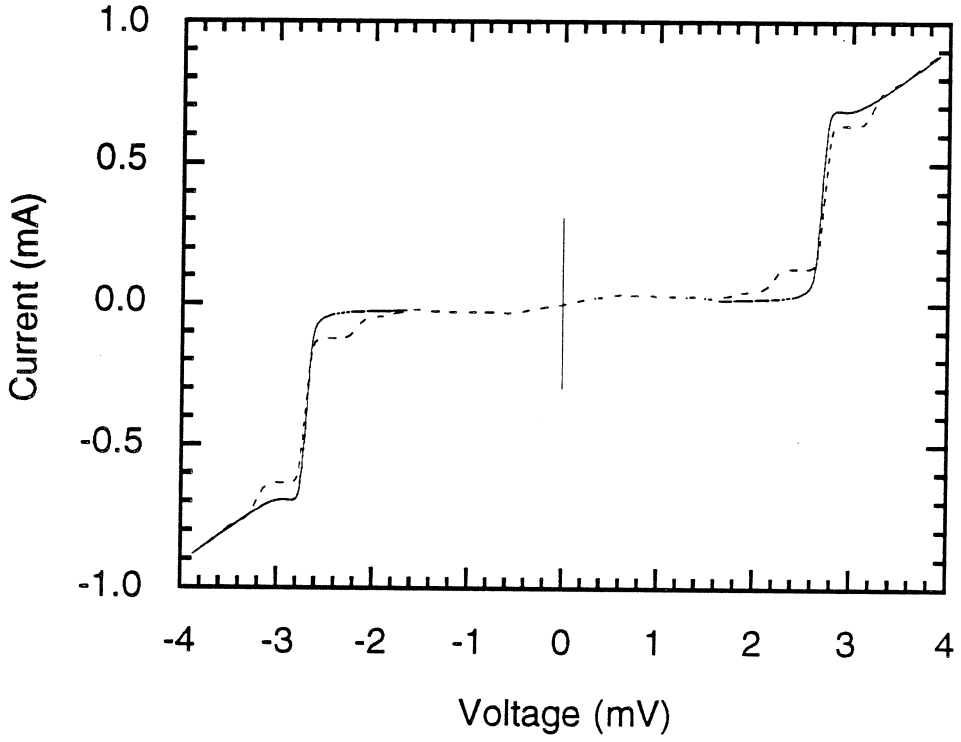

Fig. 8: The detector junction current-voltage curve with no array bias current (solid line), and with the array bias current set for maximum observed power (dashed line).

The distributed arrays produced detectable power when tested. The DC voltage across an array biased to produce power accurately determines the frequency of the oscillations. The voltage measurements were made using the four probe technique across the array while it is oscillating. All of the arrays oscillated at frequencies somewhat higher than the designed frequency of 100 GHz. Figure 9 shows a histogram of the arrays tested sorted by the frequency range of their oscillations. The size of the frequency error seems to be larger than one would expect to be due to miscalculation of the electrical length of the transmission line connecting the oscillator junctions in series. We believe this observation of power at a higher frequency than the nominal design value is consistent with that observed by Lukens and coworkers.[6]

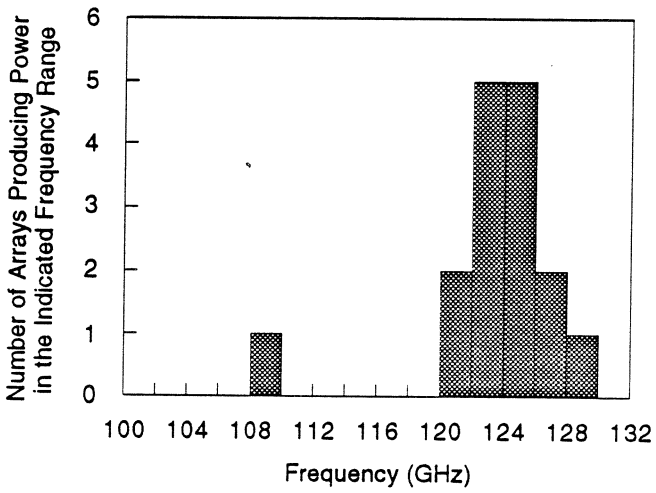

Fig. 9: The number of arrays tested which produced RF power in a given frequency range. All arrays were designed to oscillate at 100 GHz.

Conclusions

We have extended the lumped element analysis of Hadley, et al., to cover a particular case of practical importance: an oscillator array with optimum β_C feeding a complex load impedance. We find wide parameter ranges of stable, in-phase operation of oscillator elements.

We have also derived the equations of motion for the distributed array, and numerically solved the equations for several particular instances of interest. We find a significant deviation from simple extrapolations of lumped element analysis. Coherence in lumped element oscillator arrays does not guarantee stable coherent operation of distributed oscillators.

We have reported the fabrication and testing of several oscillator arrays. The on-chip detection circuitry provided a realistic test of the arrays operation in an integrated superconducting circuit. We observed at least 50 nW of 125 GHz power.

Acknowledgements

It is our pleasure to acknowledge important useful discussions with Jim Lukens and his group at SUNY Stony Brook and Arnold Silver. This work was sponsored by AF Contract F 19628-86-C-0154 with the

Electromagnetics Directorate of Rome Air Development Center, funded by the Innovative Science and Technology Office of the Strategic Defense Initiative Organization.

References

1 K. Wan, A. K. Jain, and J. E. Lukens, "Submillimeter wave generation using Josephson junction arrays", Appl. Phys. Lett., 54, (18), 1805-7, (1 May 1989).

2 P. Hadley, "Dynamics of Josephson Junction Arrays", Ph.D. Dissertation, Stanford University, March 1989.

3 A. K. Jain, K. K. Likharev, J. E. Lukens, and J. E. Sauvageau, "Mutual Phase-Locking in Josephson Junction Arrays", Physics Reports, 109, 6, 309-426, (1984).

4 R. E. Jewett, "Josephson Junctions in SPICE 2G5", University of California at Berkeley, 1982.

5 A. D. Smith, R. D. Sandell, A. H. Silver, and J. F. Burch, "Chaos and Bifurcation in Josephson Voltage-Controlled Oscillators", IEEE Trans. Mag, MAG-23, 2, March 1987.

6James Lukens, "Josephson Arrays as High Frequency Sources", in *Superconducting Devices*, Edited by Steven T. Ruggiero and David. A. Rudman, Academic Press, Inc., (1990).

7A. D. Smith, et al. to be published in the Proceedings of the ASC '90.

8J. M. Murduck, J. Porter, W. Dozer, R. Sandell, J. Burch, J. Bulman, C. Dang, L. Lee, H. Chan, R. W. Simon, and A. H. Silver, "Niobium Trilayer Process for Superconducting Circuits", IEEE Trans. Magn. **25**, 1139 (1989).

9John R. Tucker, "Quantum Limited Detection in Tunnel Junction Mixers", IEEE Journal of Quantum Electronics, **11**, 1234, (1979).